Salim, S. G. R., Fox, N. P., Hartree, W. S., Woolliams, E. R., Sun, T. & Grattan, K. T. V. (2011). Stray light correction for diode-array-based spectrometers using a monochromator. Applied Optics, 50(26), pp. 5130-5138. doi: 10.1364/AO.50.005130

Stray light correction for diode-array-based spectrometers using a monochromator

Saber G. R. Salim,[1,2,3,*] Nigel P. Fox,[2] William S. Hartree,[2] Emma R. Woolliams,[2] Tong Sun,[3] and Kenneth T. V. Grattan[3]

[1]National Institute of Standards (NIS), Tersa Street, El-Haram, P.O. Box 136, Giza 12211, Egypt

[2]National Physical Laboratory (NPL), Hampton Road, Teddington, Middlesex, TW11 0LW, UK

[3]City University London, Northampton Square, London, EC1V 0HB, UK

*Corresponding author: saber.salim@nis.sci.eg

Photodiode-array-based spectrometers are increasingly being used in a wide variety of applications. However, the signal measured by this type of instrument often is not what is anticipated by the user and is often subject to contamination from stray light. This paper describes an efficient and low-cost stray light correction approach based on a relatively simple system using a monochromator-based source. The paper further discusses the limitations of using a monochromator instead of a laser, as used by previous researchers, and its impact on the quality of the stray light correction. The reliability and robustness of the stray light correction matrix generated have been studied and are also reported.

1. Introduction

A photodiode-array-based spectrometer can be defined as a dispersive instrument with multiple optical sensors that enables simultaneous acquisition of the radiant flux over a particular spectral range [1]. These instruments are in general characterized by their small size, light weight, and low cost. In addition, they have the key advantage of capturing a spectrally resolved signal over a wide spectral range in a very short time compared to many mechanical scanning spectrometers. This has led to their widespread use in applications where signals are low, unstable, or short lived. Diode array spectrometers are becoming the preferred tool for many applications using optical radiation, for example, in remote sensing, spectroscopy, astrophysics, analytical chemistry, health, and process control [2–5].

Although such spectrometers have many advantages, they almost always suffer from stray light—arising from situations where the measured spectrally resolved signal is contaminated with radiation of a nominally different spectral content. A well-designed spectrometer, fitted with a high-quality diffraction medium (usually a grating), will minimize stray light, but it rarely will do so adequately. Further improvement can be obtained by using "cut-on" filters (usually glasses with a spectrally sharp transition between high absorption and high transmittance, e.g., RG 665 glass from Schott) in front of the array detector to remove higher order diffraction effects. However, even in the best spectrometers, the stray light value measured at any pixel, obtained from a monochromatic source of a different wavelength, is of the order of 10^{-5} of the true in-band (IB) monochromatic signal. While small for a monochromatic source, this value can be a serious problem when a broadband source is being measured, as each "wavelength" emitted by the source produces stray light at a level of 10^{-5} at each pixel, results in a cumulative effect,

which has a significant impact on the final signal measured. This issue can be an even greater problem for any part of the spectrum where the desired signal is relatively weak, e.g., the blue for an incandescent lamp as compared to the red, for example.

The responsivity of a diode array spectrometer is usually obtained by calibration against a reference standard source, such as a tungsten lamp of known spectral distribution. It is subsequently used to detect radiation from sources or surfaces with different spectral distributions, such as oceans, sky, and land surfaces and sources such as lasers or LEDs. Because of the spectral mismatch between the calibration source and the source under test, the stray light signal is not canceled out by a simple substitution process. This limits the accuracy and reliability of spectral measurements carried out using an array spectrometer. It is thus essential that the stray light performance of such instruments is assessed properly for each application, particularly for those requiring high accuracy and where necessary and possible, corrections for the presence of stray light are made.

2. Sources of Stray Light inside an Array Spectrometer

Ideally, each pixel in an array spectrometer should detect only the radiation with a spectral content characterized by those wavelengths directed to it by the dispersing element, without sensing any contribution from light at any other wavelengths. In practice, there is always some response due to other wavelengths (i.e., what is termed "stray light") that ideally should not be present but is. The major sources of stray light inside diode array spectrometers can be summarized as follows:

i. **Scattered light from the internal walls and input optics of the spectrometer.** Light that deviates from the desired optical path and light from negative, zero and higher orders can be reflected onto the array detector from the internal walls or other components of the spectrometer.

ii. **Dispersive element, usually a diffraction grating.** Diffraction grating limitations are more apparent in photodiode array spectrometers than in mechanical scanning spectrometers: higher order diffraction signals "pollute" the desired first-order diffraction, and ruling imperfections in the grating grooves and coatings may lead to further scattering effects [6]. In addition, "cut-on" filters are used in front of the array elements to eliminate higher order diffraction signals, but these filters themselves become sources of stray light.

iii. **Interreflections.** Some light is always reflected by each optical detector element onto other parts of the spectrometer. If cut-on filters are used, some of this reflected light will be rereflected back onto the sensor or its neighboring pixels. This is termed "near-field stray light" and appears as a "hump" near the profile of a monochromatic light source. This near-field signal can be quite significant, as observed by Zong *et al.* [7].

iv. **Light coupling.** Design constraints of the spectrometer, particularly related to the way that light is coupled into it, may also be a source of stray light. This may occur, for instance, when using a fiber with a larger numerical aperture (NA) than that specified by the design increases stray light levels.

3. Existing Stray Light Correction Methods

Several approaches have been suggested to evaluate and correct for the spectral effects of stray light in diode array spectrometers. One such approach, proposed by Brown *et al.* in 2003 [1], depends on characterizing the slit scattering function (SSF) (proposed by Kostkowski [8]). The SSF is commonly used for stray light evaluation in mechanical scanning spectrometers, where the monochromator is held at a particular wavelength setting then illuminated by a series of monochromatic wavelengths.

Another more comprehensive (and relatively simple approach) has been proposed by Zong *et al.* [7]. The method uses a spectrally tunable laser source to measure the full spectrometer response for different monochromatic input wavelengths. At each wavelength (λ_j), the spectrometer has a spectral line spread function (LSF) denoted by f_{LSF}, which represents the response of each pixel to this wavelength. Because the incident light in such a case is monochromatic, any response at pixels outside the IB region, as detected by the spectrometer, can be considered as stray light. This stray light signal can be evaluated by dividing the response at each pixel i by the integration of the IB signal after normalizing the value of f_{LSF}.

The resultant function is called the spectral stray light distribution function ($d_{i,j}$), and this can be expressed as [7]

$$d_{i,j} = \frac{f_{\mathrm{LSF},i,j}}{\sum_{i \in \mathrm{IB}} f_{\mathrm{LSF},i,j}}, \qquad i \notin \mathrm{IB}, \tag{1}$$

where $d_{i,j}$ is the spectral stray light signal at pixel i due to a monochromatic light that shows its maximum at pixel j. An $n \times n$ stray light distribution matrix (D) can be formed by populating the matrix with the individual elements, $d_{i,j}$.

When light from a broadband source illuminates the photodiode array, the measured signal (Y_{meas}) can be expressed as the sum of the signal for no stray light (Y_{IB}) plus the contribution of the stray light to this signal:

$$Y_{\mathrm{meas}} = Y_{\mathrm{IB}} + D \cdot Y_{\mathrm{IB}} = [1 + D] Y_{\mathrm{IB}} = A Y_{\mathrm{IB}}, \tag{2}$$

where A is called the square coefficient matrix. In such a case, the correction obtained by Zong *et al.* [7] is given by

$$Y_{\mathrm{IB}} = A^{-1} Y_{\mathrm{meas}} = C Y_{\mathrm{meas}}, \tag{3}$$

where C is called the stray light correction matrix, which is the inverse of A.

In practice, the stray light distribution matrix (D) can be obtained from knowledge of a reasonable subset of the elements, $d_{i,j}$ measured at different wavelengths across the spectral range of the spectrometer. The remainder of the n number of columns can be interpolated and, with care, extrapolated.

In the work carried out by Zong *et al.* [7], a tunable laser was used to determine the spectrometer response to a set of wavelengths across its range of operation to obtain the inputs for the matrix D.

The work carried out and reported in this paper has aimed to demonstrate how this approach could be further simplified through the use of monochromator-generated radiation.

4. Monochromator-Based Correction

Unlike spectrally tunable lasers, monochromators are widely available at relatively low cost and are easy to use. They are readily accessible, not only to national metrology institutes but also to commercial organizations. A monochromator-based approach has previously been implemented, as presented by Lenhard *et al.* [9], but this paper explores this concept in significantly more detail. While monochromators have a number of operational advantages, they also suffer from some issues that may limit the overall performance achievable, e.g., the source bandwidth, the output radiation levels, and the presence of inherent stray light. There is an interrelationship between these factors; for example, output levels can be increased by using larger bandwidths but this, of course, compromises spectral resolution. This work reviews these limitations and their impact on the correction obtained.

A. System Bandpass Function

1. *Calculating the System Response Function*

When a laser source is used, the overall system bandpass function will be essentially that of the spectrometer. For a monochromator-based method, the system bandpass function is given by a combination of the monochromator and spectrometer bandpass functions.

This interaction between the diode array spectrometer and monochromator was studied using a simple model that allowed an estimation of the shape of the overall system bandwidth and the signal level. The spectrometer bandpass function was taken to be that measured using an He–Ne laser at 632.8 nm, and the monochromator bandpass function was assumed to be a triangular function of 1 nm FWHM. The bandpass functions of the spectrometer and monochromator were normalized to unity at their maxima, as shown in Fig. 1.

Each point on the monochromator bandpass function was assumed to result in the same spectrometer bandpass profile as if it were a laser, i.e., being equivalent to the output of the He–Ne laser, as shown in Fig. 2.

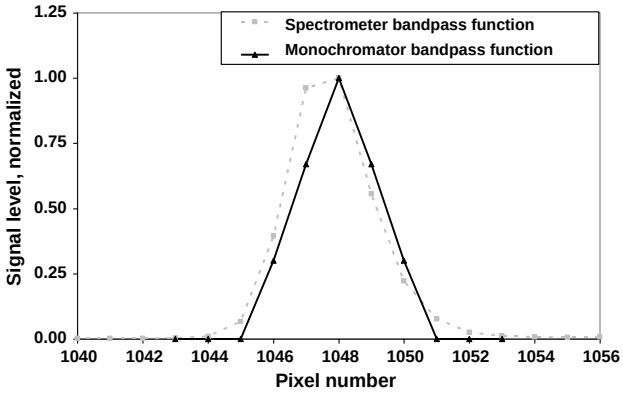

Fig. 1. Spectrometer bandpass and the monochromator bandpass functions—the X axis is replaced by the pixel order inside the array detector rather than the wavelength.

The spectrometer signal at a particular pixel is thus the sum of the pixel responses to each point on the monochromator bandpass function. The darkest (black) line in Fig. 3 shows the combination of the monochromator and the spectrometer bandpasses, as calculated by the model. The calculated resultant system bandpass (~1.6 nm FWHM) is slightly wider than the spectrometer bandpass function obtained using the laser (~1.2 nm FWHM) and the monochromator bandpass profile (~1 nm FWHM).

It should be noted that this approach can be created by convolving the monochromator spectrometer bandpass function $x(n)$ and the spectrometer bandpass function, as described elsewhere in the literature [10]. The convolution $Y(n)$ can simply be written as

$$Y(n) = x(n) * y(n) = \sum_{i=-n}^{n} x(i)y(n-i), \qquad (4)$$

where n is the pixel number and i is an integer in this case. This equation is numerically intensive to evaluate; therefore, it can be converted into a multiplication by using a FFT such as

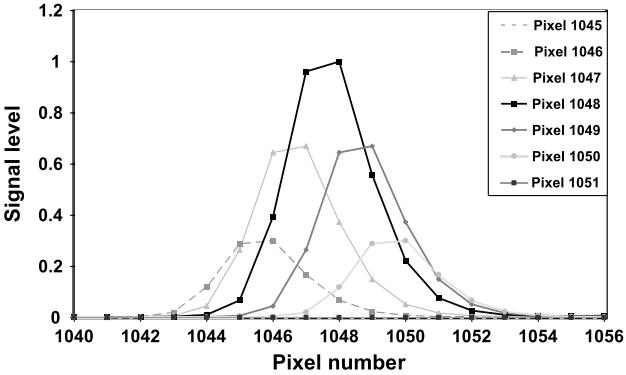

Fig. 2. Response of the spectrometer to every point on the monochromator bandpass function.

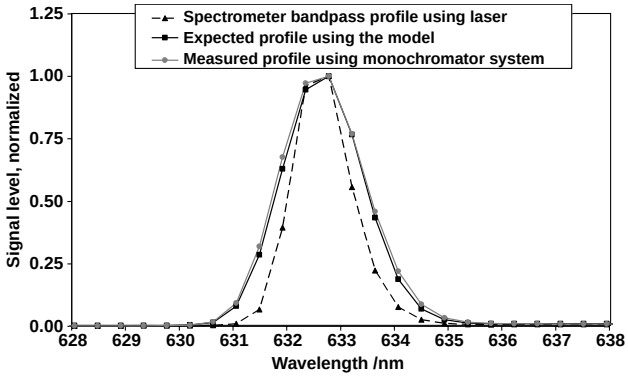

Fig. 3. Convolution of the spectrometer and the monochromator bandpass functions: model and experimental results.

$$Y = \mathrm{IFFT}(\mathrm{FFT}(x)\mathrm{FFT}(y)). \tag{5}$$

Although this approach is straightforward, it may be necessary to apply windows (e.g., Hanning) to the functions, which may affect the profile of the bandwidth in the final result. In addition, it may be required to remesh the functions so they are on the same grid.

The applicability of the model was confirmed experimentally by measuring the bandpass function of the instrument using the system shown in Fig. 4. The measured bandpass profile was found to be very close to that calculated by the model (the dark gray line shown in Fig. 3).

Even with wider monochromator bandpass values (of 2 and 3 nm—these are wider than the spectrometer bandpass), the system bandpass was found to be only slightly larger than the monochromator bandpass. However, the best results were obtained experimentally with the slit width of the monochromator set to be as narrow as possible, to make the system bandwidth and spectrometer bandwidth very close to each other in value—although there will be a compromise in this choice when the signal levels are small.

2. *Bandpass Profile and Stray Light Calculations*

The chosen width of the "IB" region affects the resultant stray light correction matrix, as the spectrometer response at each pixel element is divided by the integration over the IB region. The width of the IB region increases at higher wavelengths due to the increased bandwidth of the spectrometer, also the level of the near-field stray light has been found to vary across the spectrometer spectral range. Therefore, it is seen as important to take these considerations into account when defining the IB region, and this was done.

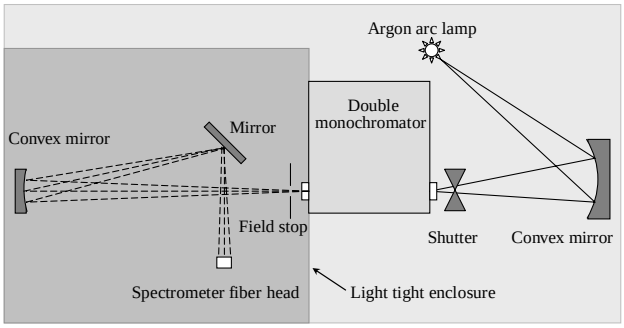

Fig. 4. Monochromator-based stray light correction system.

B. Stray Light Signal inside the Monochromator

Unlike a laser, monochromators will have their own stray light. Therefore, the stray light correction should be carried out using a double grating monochromator in which the associated internal stray light is typically of the order of $\sim 10^{-6}$. Ideally, the residual stray light should be completely prevented from entering the spectrometer, but this is not easily achieved in practice. However, the effect of this small level of monochromator-based stray light is thought to be negligible in the operation of the system.

5. Experiment and Setup

The experimental system used in this work, shown in Fig. 4 and based largely on the NPL spectral responsivity facility, was set up to conduct the stray light correction. An argon arc lamp, which has a relatively high spectral emission (especially in the UV region), was used. The light emitted from the lamp was focused onto the entrance slit of a double monochromator using a convex mirror.

The monochromator output light was directed by convex and plane mirrors to the lens attached to the SMA connection of the spectrometer fiber. This lens is used to define the field of view of the spectrometer. The f number of the beam could be adjusted using a field stop located beyond the exit slit of the monochromator. During the measurements carried out, care was taken to ensure that the light overfilled the lens aperture to mimic normal operation. The spectrometer fiber lens was aligned to maximize the collection of light; this occurred when the spot (representing the optical beam) on the plane mirror was located in the field of view of the fiber lens.

Higher order diffraction was suppressed during the spectral scan of the monochromator by the use of cut-on filters inside the monochromator facility, operating at wavelengths of 390 and 670 nm. This in turn ensured a further reduction of the stray light inside the monochromator.

Below a wavelength of 650 nm, gratings with a blaze of 500 nm were used, while for longer wavelengths, gratings with a blaze of 700 nm were employed in this work. The lamp current was optimized to ensure that a reasonable signal level was obtained over all the spectral regions studied.

The spectrometer used for the tests carried out is a commercial instrument that employs a high-sensitivity miniphotodiode array manufactured by Hamamatsu (type C10083CAH), and the array detector is a 2048 pixel element back-thinned silicon photodiode array. The spectrometer covers the spectral range from 208 to 1078 nm; as this also covers

most of the silicon detector responsivity range, errors due to stray light from wavelengths outside this range were considered negligible. The analog-to-digital converter used with the spectrometer has 16 bit resolution, which means that one single count is 1.52×10^{-5} of the maximum number of counts (65,536). To detect stray light values less than this level, the spectrometer output signal was sampled 1000 times, ensuring sufficient resolution in the stray light measurement (i.e., a signal level could be obtained to sufficient significant figures) to evaluate the actual low-level stray light present.

To study the impact of the monochromator bandwidth on the efficiency of the stray light correction matrix, the column vector $d_{i,j}$ was evaluated by the measurements at 555 nm, for four different monochromator bandwidths (1, 2, 3, and 4 nm), and the results obtained are shown in Fig. 5.

For the bulk of the spectrum, it can be seen that the results obtained are nearly identical. However, the use of narrower bandwidths is required to determine the stray light levels at the pixels immediately adjacent to the IB region. This means that to obtain a measurable signal, priority should be given to either increasing the source signal or using a higher integration time, rather than simply using a wider monochromator bandwidth. The monochromator slit width was therefore adjusted to give a 1 nm bandwidth, and the lamp power increased to ensure a reasonable signal-to-noise ratio was obtained. The same bandwidth was used over the entire wavelength domain to ensure consistent results for the values given by $d_{i,j}$.

The nonlinearity performance of the spectrometer has been found to be affected by using different integration times and different source intensities [11]. The impact of these two factors on the values of the spectral stray light distribution function has been studied. The effect of using different integration times was studied at a wavelength of 850 nm, where integration times of 10, 20, and 30 ms were used to tune the spectrometer signal level from a maximum of 20,000 counts to nearly 60,000 counts, while keeping a fixed source intensity. No noticeable differences in the resultant values of $d_{i,j}$ were observed, other

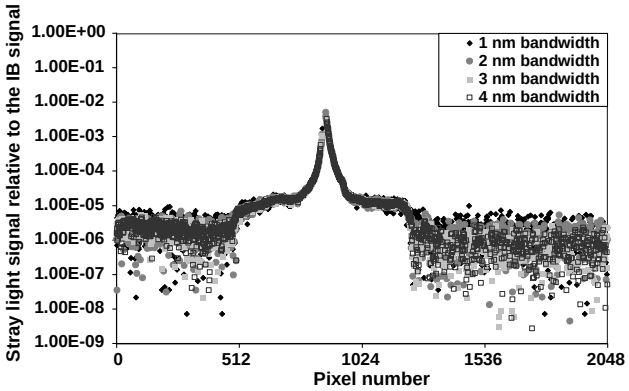

Fig. 5. Spectral stray light distribution function for different monochromator bandwidths.

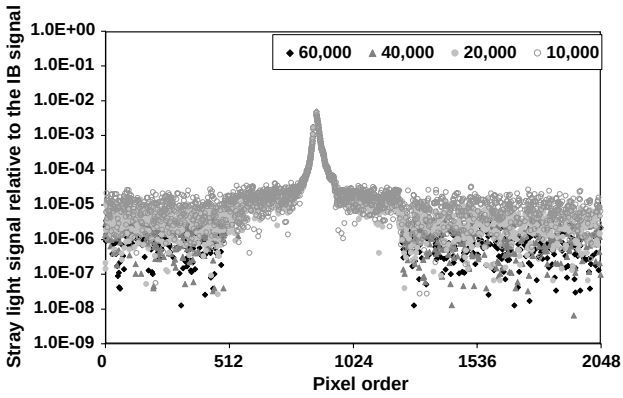

Fig. 6. Spectral stray light distribution function for different irradiance levels.

than obtaining improved noise characteristics for the use of higher integration times. The effect of using different source intensities was studied at a wavelength of 550 nm, while keeping a fixed integration time. The results of this effect are shown in Fig. 6. The measured stray light was observed to increase slightly when low signal levels were used, but there was no noticeable change between the stray light level observed at signal levels of 40,000 and 60,000 counts. This can be explained in terms of the relative response of each pixel, which is slightly higher at lower signal levels. The effect is generally small, but to ensure consistency, all subsequent analysis was done with signal levels greater than 20,000 counts.

6. Results

A. Spectral Stray Light Distribution Function

The spectrometer signal was measured at 5 nm intervals over the whole spectral range. At each measured wavelength, a corresponding dark signal was also recorded. The dark-corrected spectrometer signal was normalized to the maximum level to obtain the value of f_{LSF}. Although all the spectral LSFs were measured at high integration times, some pixels gave negative values as a result of noise in the dark and light signals. However, the number of such pixels was, in general, small, as were the values of the (negative) numbers they gave. The values of f_{LSF} have been calculated as a result of repeated measurements at a wavelength of 550 nm, following which the results obtained were compared. It was noticed that when the experiment was repeated, these negative values were not repeatable for these specific pixels, thereby confirming that these results were simply due to noise. Ideally, noise with both signs (negative and positive) should be removed from the "real" signal; however, it is not possible to distinguish noise with a positive sign from the stray light signal. Therefore, it was decided in the analysis to replace any negative values obtained with a zero, as they did not represent a real stray light signal. Further justification for this was that, in addition, leaving the negative values may result in "undercorrecting" the stray light

signal. It is important to note that a "rolling average" signal to reduce noise should be avoided, as this was found to result in poorer correction than the approach suggested.

The IB region was determined manually by carefully selecting the pixels defining the "wings" before integration. The spectrometer signal at each pixel was then divided by the integral of the IB signal to obtain the values of $d_{i,j}$ required.

The values of f_{LSF} obtained showed no signal for input wavelengths below 270 nm despite a significant output from the monochromator (as measured by a reference photodiode). This lack of a spectrometer response was attributed to the very poor transmittance of the lens in this region. As a consequence, zero values for f_{LSF} were used in the spectral range below 270 nm.

With input wavelengths from 270 to 340 nm, there was some noticeable second-order diffraction light, as shown by $d_{i,j}$ and illustrated by the black line in Fig. 7. This second-order diffraction was not visible for longer wavelengths. The stray light levels were also higher for wavelengths corresponding to pixels located at both ends of the spectrometer detector array than for those pixels in the middle.

By comparison to Fig. 7, Fig. 8 shows an increased IB width at wavelengths around 500 and 700 nm due to an increase in the near-field stray light signal. A finer scanning of the input wavelength, at 1 nm intervals, was used to examine thoroughly the stray light levels in these regions. Figure 9 shows the values obtained for f_{LSF} for inputs at wavelengths of around 507.6 and 709.5 nm (corresponding to pixel numbers 753 and 1225), which represent the observed center of this increased IB width.

According to the manufacturer's literature, there are three cut-on filters, which are used to block the higher order diffraction signals (these are types WG305, GG475, and RG665). The boundaries between the filters occur at pixels that correspond to wavelengths of 507.6 and 709.5 nm. This is likely to result in an increase in the scattered light in the region of these pixels and hence the broadening in the stray light profile. The presence of these filters also explains the reduced signal level in the vicinity

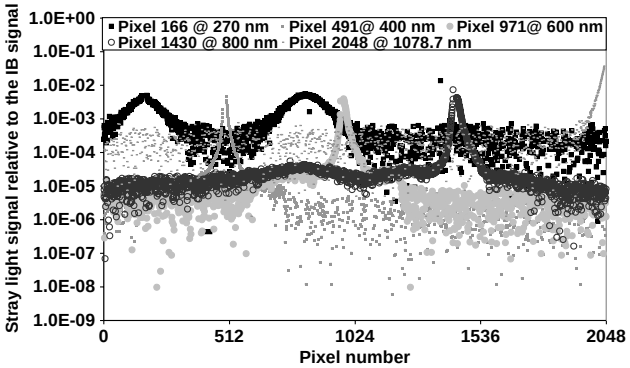

Fig. 7. Spectral stray light distribution function ($d_{i,j}$) at different input wavelengths.

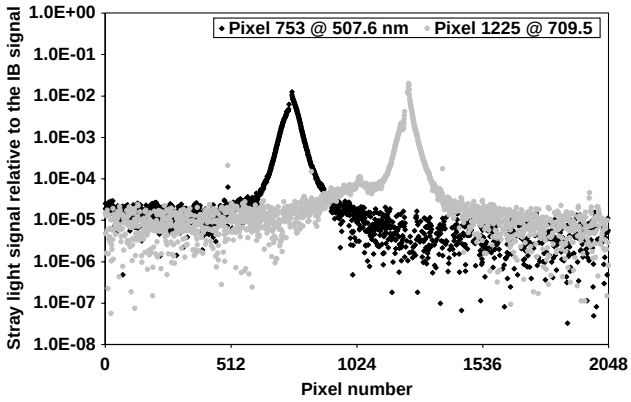

Fig. 8. Spectral stray light distribution function ($d_{i,j}$) at 507.6 and 709.5 nm input wavelengths.

of these wavelengths when the spectrometer is exposed to light from a broadband source.

Because of this, the spectral ranges around 507 and 709 nm were measured at input spectral intervals of 1 nm so as to show the exact spectral distribution of the stray light around those pixels.

B. Stray Light Correction Matrix

The stray light correction algorithm used is required to ensure that it not only provides a good estimate of stray light but also that it does not alter any other characteristic of the spectrometer under test. For example, a poor correction matrix may lead to a decrease in the apparent signal-to-noise level of the spectrometer. To test the reliability of the stray light correction matrix, measurements of two stray light sensitive sources were analyzed, while modeling was also performed to understand the sensitivity to noise.

1. Performance of the Stray Light Correction Matrix

Having calculated $d_{i,j}$ at the pixels where measurements were made, values for $d_{i,j}$ in other regions were interpolated using a MATLAB routine within the stray light correction software [12]. To deliver an accurate near-field correction, $d_{i,j}$ was interpolated along the matrix diagonals (parallel to the matrix main diagonal).

The stray light distribution matrix is shown in Fig. 10. The figure further shows an increased near-field stray light signal in the IR region. The second-order diffraction stray light is also shown in the figure at the shorter wavelengths.

The effectiveness of the stray light correction matrix to achieve a suitable correction for the stray light was tested using two sources: a low argon pressure lamp and a tungsten halogen lamp, with the output filtered with a 630 nm cut-on filter. In each case, the measured signal was normalized to the maximum before the stray light correction was applied.

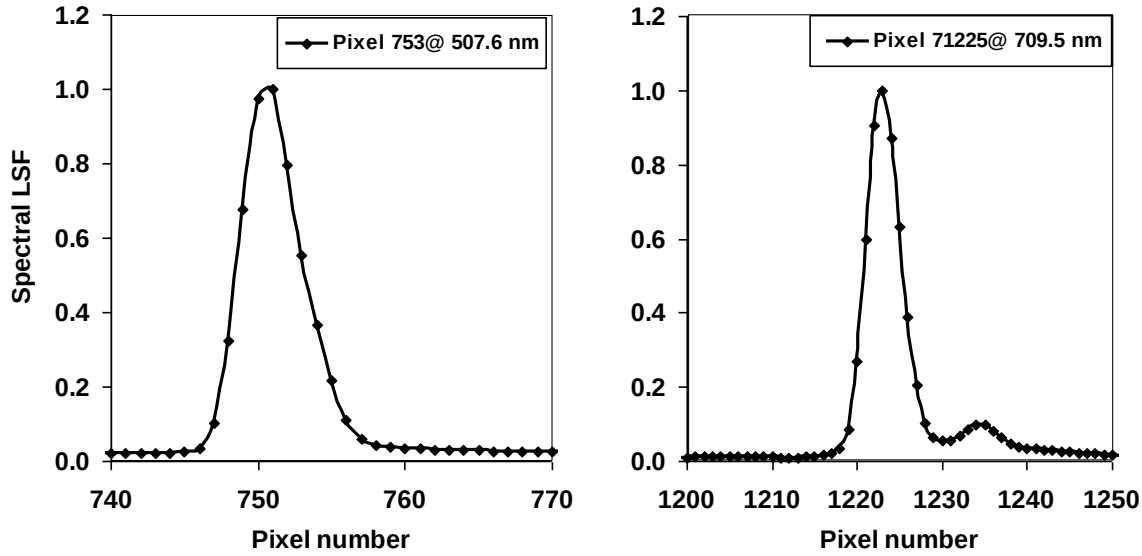

Fig. 9. Spectral LSF (f_{LSF}) at 507.6 and 709.5 nm input wavelengths.

The cut-on filter signals before and after correction was applied are shown in Fig. 11 for the filtered lamp and Fig. 12 for the spectral lines of the argon lamp. Figure 11 shows a signal level $<10^{-6}$ below the filter cut-on wavelength and a reduced signal level in the IR region where stray light also would be expected. Figure 12 shows the use of the correction has resulted in a nearly ideal shape of the spectral profile of the selected argon lines. In addition, the stray light in the far field has also been reduced by nearly 1 order of magnitude.

Having obtained these high-quality results, the reliability of the correction matrix when using a smaller number of input data points was evaluated. In this example, the resolution of the scanning of the input wavelength was reduced to 20 nm intervals, contrasting with the 5 nm interval previously used. For the highly sensitive regions at wavelengths around 507 and 709 nm, data taken every 3 nm (contrasting with the previous 1 nm) were used. The new stray light correction matrix showed identical results to those obtained previously with the whole set of measured points. Thus, relatively few characterization wavelengths are required for the determination of an accurate stray light correction matrix; however, where there are anomalies, e.g., where cut-on filters may overlap, it is clear that a more detailed spectral evaluation is required.

2. *Matrix Sensitivity Coefficient*

For a linear algebraic system, such as that represented by Eq. (2), the sensitivity of the solution (Y_{IB}) to changes in the measured signal given by the spectrometer (Y_{meas}) and the square coefficient matrix (A) can be studied using the condition number of the square coefficient matrix A [13]. The condition number is defined as the product of the norm of A and the norm of A^{-1}. This number is always greater than or equal to 1. If it is close to 1, this means that the matrix inverse can be calculated with high accuracy; however, if it is much larger, this means that the matrix inverse is "ill-conditioned" and cannot be calculated accurately. A large condition number will mean the correction is more sensitive to measurement errors in the determination of the stray light correction matrix, and less able to reproduce small

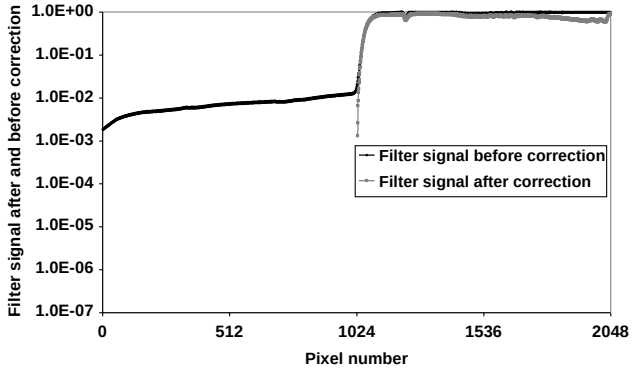

Fig. 10. 3D stray light distribution matrix obtained by using diagonal interpolation.

Fig. 11. Cut-on filter signal before and after stray light correction.

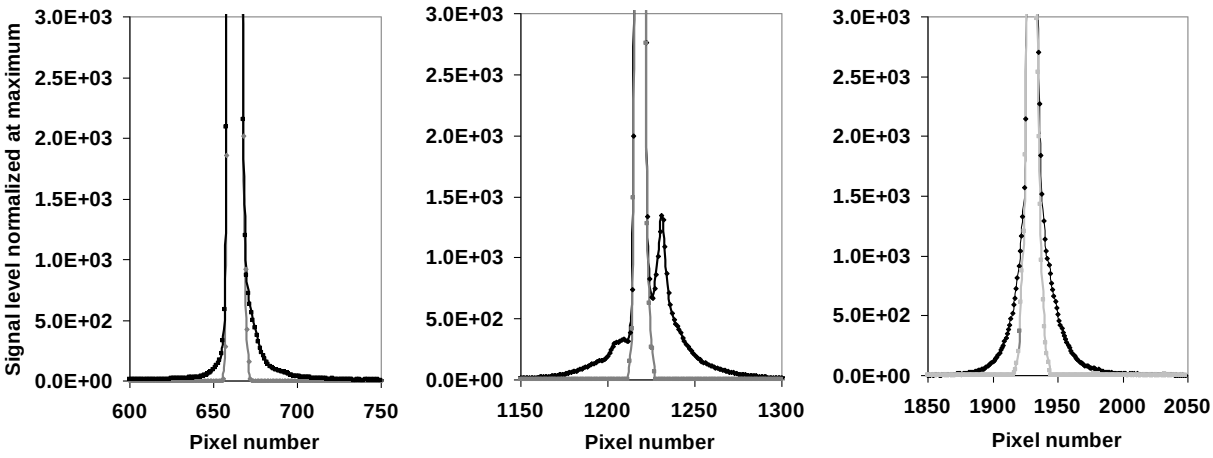

Fig. 12. Performance of the stray light correction matrix at the 407.2, 706.7, and 1025.4 nm argon lines.

variations in the spectrum being recovered. A condition number equal to infinity means that the matrix is noninvertible.

For the correction of the spectrometer used in this work, the condition number of the square coefficient number was found to be 1.86, which is somewhat higher than the value 1.07 obtained by Zong *et al.* [7]. This is likely mainly to be due to the fact that this stray light correction matrix was zero for input wavelengths below 270 nm (due to the lens transmittance), and, in addition, the signal also had relatively high stray light signals at longer wavelengths.

As the condition number was somewhat higher, it was considered necessary to check the sensitivity of Y_{IB} to variations in Y_{meas}. A spectral structure of periodically oscillating amplitude of $\pm 0.5\%$ of the value of Y_{meas} was deliberately added to Y_{meas} for a tungsten lamp signal, and Y_{IB} was calculated before and after adding this periodic oscillation. The difference between the two output spectra showed the same periodic spectral structure with a corresponding oscillating amplitude of $\pm 0.56\%$ at 400 nm increasing gradually to $\pm 0.72\%$ at 1078 nm. In addition, random noise of relative amplitude within $\pm 0.5\%$ was added to Y_{meas}, and Y_{IB} was recalculated before and after adding this random noise. The difference between the two output spectra was found to be similar to the values observed when adding the periodic oscillation to Y_{meas}. These tests show that the stray light correction matrix causes only minor distortions to small changes in the spectrum being measured, and the condition number for this spectrometer is acceptable.

7. Summary

This paper has shown that one of the major sources of uncertainty that limits the performance of the diode-array-based spectrometers—stray light—can be accurately corrected with a relatively fast procedure using cheap and readily available monochromators, with results comparable to those obtained using tunable lasers. The work reported in this paper has described the sensitivity of the stray light characterization method to both the measurement system and subsequent mathematical evaluation processes. It also has shown that the number of measurement points needed for the correction can be reduced significantly without impacting on the overall performance of the system.

The application of these procedures could be used to make it possible for low-cost spectrometers of this nature to move from being useful spectral monitoring devices to high-performance optical spectroradiometers capable of transforming optical radiation measurement in a wide variety of applications that currently are limited by the achievable accuracy or by the lack of flexibility arising due to large immovable instrumentation.

The authors would like to acknowledge the contribution of Ian Smith of the NPL Scientific Computing Team for his help in writing the MATLAB code for diagonal interpolation and Andrew Levick for his valuable comments. One of the authors (S. Salim) gratefully acknowledges the award of a fellowship from the Cultural Affairs & Scientific Missions Sector, Egypt. This work was supported by the National Measurement Office of the UK Department "Business, Innovations, and Skills (BIS)."

References

1. S. B. Brown, B. C. Johnson, M. E. Feinholz, M. A. Yarbrough, S. J. Flora, K. R. Lykke, and D. K. Clark, "Stray-light correction algorithm for spectrographs," Metrologia **40**, S81–S84 (2003).
2. M. Belluso, M. C. Mazzillo, S. Billotta, S. Scuderi, A. Calí, A. Micciché, M. C. Timpanaro, D. Sanfilippo, P. G. Fallica, E. Sciacca, S. Lombardo, and A. Morabito, "SPAD array detectors for astrophysical applications," Mem. S. A. It. Suppl. **9**, 430–432 (2006).
3. S. G. R. Salim, N. P. Fox, E. R. Woolliams, R. Winkler, H. M. Pegrum, T. Sun, and K. T. V. Grattan, "Use of eutectic fixed points to characterize a spectrometer for earth observations," Int. J. Thermophys. **28**, 2041–2048 (2007).
4. H. Shen, T. J. Cardwell, and R. W. Cattrall, "The application of a chemical sensor array detector in ion chromatography for the determination of Na^+, $NH4^+$, K^+, $Mg2^+$ and $Ca2^+$ in water samples," Analyst **123**, 2181–2184 (1998).

5. S. S. Vogt, R. G. Tull, and P. Kelton, "Self-scanned photodiode array: high performance operation in high dispersion astronomical spectrophotometry," Appl. Opt. **17**, 574–592 (1978).
6. C. Palmer, *Diffraction Grating Handbook* (Thermo RGL, 2002).
7. Y. Zong, S. B. Brown, B. C. Johnson, K. R. Lykke, and Y. Ohno, "Simple spectral stray light correction method for array spectroradiometers," Appl. Opt. **45**, 1111–1119 (2006).
8. H. J. Kostkowski, *Reliable Spectroradiometry* (Spectroradiometry Consulting, 1997).
9. K. Lenhard, P. Gege, and M. Damm, "Implementation of algorithmic correction of stray light in a pushbroom hyperspectral sensor," in *6th EARSeL Imaging Spectroscopy SIG Workshop* (EARSeL, 2009), http://www.earsel6th.tau.ac.il/~earsel6/CD/PDF/earsel-PROCEEDINGS/3035%20Lenhard.pdf.
10. N. Ronald, Bracewell, *The Fourier Transform and Its Applications* (McGraw-Hill Science Engineering, 1999).
11. S. G. R. Salim, N. P. Fox, E. Theocharous, S. Tong, and K. T. V. Grattan, "Temperature and nonlinearity corrections for a photodiode array spectrometer used in the field," Appl. Opt. **50**, 866–875 (2011).
12. MATLAB version 6.5.1. Natick, Mass., The MathWorks, Inc. (2003).
13. C. Moler, *Numerical Computing with MATLAB, Linear Equations* (Society for Industrial and Applied Mathematics, 2004).